

## Interaction Mechanism between Zn and Passivated Stainless Steel

Yan Zhao<sup>1</sup>, Di-yao Zhang<sup>1</sup>, Jian-jun Guan<sup>1,\*</sup>, Feng Liu<sup>1</sup>, Ping Liang<sup>1</sup>, Cong-qian Cheng<sup>2</sup>, Jie Zhao<sup>2</sup>

<sup>1</sup> School of Mechanical Engineering, Liaoning Shihua University, Fushun 113001, Liaoning, China

<sup>2</sup> School of Materials Science and Engineering, Dalian University of Technology, Dalian 116085, Liaoning, China

\*E-mail: [jjguan-hj@163.com](mailto:jjguan-hj@163.com)

Received: 17 September 2018 / Accepted: 12 November 2018 / Published: 30 November 2018

---

This study investigated the interaction between solid Zn and passivated stainless steel. The effect of passivation film on the interaction mechanism of Zn and stainless steel surface was determined. The cross section morphology and the chemical compositions of the intermetallics (IMC) were detected by scanning electron microscopy (SEM) and energy dispersive X-ray spectrometer (EDX). The composition and integrity of the passivation films were identified by X-ray photoelectron spectroscopy (XPS) and Mott-Schottky electrochemical analysis. Results showed that solid Zn reacted with stainless steel by forming interfacial columnar  $\delta$  phase (Fe, Cr, Ni) $Zn_{10}$  with tiny granule  $\zeta$  phase (Fe, Cr, Ni) $Zn_{13}$  IMCs. The reaction was hindered by the chemical passivation film and the native oxide film grown in air; the influence of the former is significantly higher than that of the latter. The passivation films were composed of Fe-rich and Cr-rich oxides and hydroxides. The chemical passivation film was richer in Cr oxides and hydroxides and had higher integrity than the native oxide film. The IMCs formed between the low-melting-point-metal and stainless steel can be attributed to the incomplete passivation films, which impeded the compound layer growth to some extent. The passivation film served as a physical barrier between solid Zn and stainless steel.

---

**Keywords:** Solid Zn, Stainless steel, Passivation, XPS, Mott-Schottky

### 1. INTRODUCTION

At high temperature, the compatibility of solid metal and low-melting point metal is an important issue to ensure the safe operation of nuclear power equipment. Corrosion failure or brittle fracture will occur due to low-melting point metal penetrating into the solid-metal grain boundary [1, 2]. As an addition element in coating, the oxidation of low-melting point metal Zn or its diffusion along the steel provides protection capability reduction of coating to the steel material. The nuclear components can be

contaminated by Zn due to the coating degradation. The safe usages of facilities in nuclear plants is threatened under high temperature and high pressure service environment for more than 10 years; these threats include water contamination in the primary circuit caused by coating inside the nuclear storage tank and abnormal operation of turbine due to coating failure in the main fuel tank [3]. Therefore, the interaction between Zn and materials in nuclear power equipment should be given considerable attention.

For the interaction between Zn and metal materials, the effect of the intermetallics for the reaction of Zn with alloy steel on the microstructure and properties has been studied. Corrosion resistance of nitrided stainless steel and cast iron in liquid low-melting point metal was studied by Hu et al [4]. The microstructure and mechanical properties of galvanized coating on the duplex steel were reported by Song et al [5]. Reumont et al [6] studied the fatigue properties and failure mechanism of galvanized IF steel. The results of Bellhouse and McDermid showed that Zn has a good wetting interface reaction with high Al and low Si phase transformation induced by the steel [7]. Ma et al. analyzed the surface morphology and corrosion resistance of the boundary of Fe-B cast steel in liquid Zn [8]. The interaction between carbon steel, cast steel and Zn was mainly reported in the literatures [9, 10], indicating that the Zn contact with carbon steel occurred via forming intermetallic compounds.

Stainless steel is widely used in nuclear power plant because of its good mechanical properties and corrosion resistance. The interaction between stainless steel and low-melting point metal Zn is rarely reported in literature. The oxide film on the stainless steel surface is an important barrier to protect the substrate from external contamination. Luo points out that the oxide film on the material surface prevents the diffusion of solid material in liquid metal [1]. Lee et al.'s research revealed that surface oxide film reduces the reaction between low-carbon steel and liquid metal [11]. Therefore, oxide film plays an important role in the interaction between low-melting point metal and solid material. The oxidation film of stainless steel can be grown by self-passivation in air environment, and the passivation film is grown by chemical passivation in industrial application [12]. However, the passivation film affects the diffusion reaction between Zn and metal atoms, such as Fe and Cr in stainless steel. This phenomenon is a scientific problem needing close attention.

In this study, the microstructure and contact degree of Fe-Zn compounds after the interaction between Zn and passivation stainless steel were analyzed. Moreover, the effects of passivation film on the interaction were studied. The characteristics of passivation film on stainless steel surface were measured by X-ray photoelectron spectroscopy (XPS) and Mott-Schottky measurements. The influence of passivation film on the diffusion reaction mechanism between Zn and metal atoms, such as Fe and Cr, was revealed. The theoretical model of interaction between Zn and passivation stainless steel was built.

## 2. EXPERIMENTAL

The material used in the experiment is 304L austenitic stainless steel (304L SS). Its the main chemical composition ( wt % ) is C 0.025 , Cr 17.59 , Ni 9.208 , Mn 1.062 , Si 0.635 , Mo 0.091 , S 0.005 , P 0.019 , the rest are Fe. The 304 SS was cut into pieces with the size of is 20 mm×15 mm×1.5 mm. The samples were successively grounded by emery paper and then rinsed with water and ethanol.

Chromaticity approach was proposed to inspect the quantity of the passive film on stainless steel. The passivation condition is based on the detection results of chromogenic inspection [13]. The preparation of stainless steel at different passivation states is shown in Table 1. The sample with rare surface passivation film after mechanical grinding were defined as the fresh surface sample. The air exposure processes were conducted by storing the samples to air for different durations after grinding. As recommended by ASME [14], oxide films after chemical passivation grew in 25vol. % HNO<sub>3</sub> solution at 50 °C for 30 min.

**Table 1.** Passivation states and preparing method for stainless steel in the work

Passivation conditions of 304L SS	Preparing method
Exposure in air for 0 h	Mechanically abrading with emery paper up to # 1200
Exposure in air for 1 h	Exposure in air for 1 h after grinding
Exposure in air for 24 h	Exposure in air for 24 h after grinding
Exposure in air for 48 h	Exposure in air for 48 h after grinding
Exposure in nitric acid	Immersing abraded 304L SS in 25 vol.% HNO <sub>3</sub> at 50 °C for 30 min

The interaction between passivation stainless steel and Zn was carried out in OTL 1200 vacuum tube furnace. Solid Zn was prepared with 100 μm thickness, and grounded up to 2000 # emery paper to remove its surface oxidation layer. Solid Zn plate and passivation stainless steel were fixed with a three-point clamp. Then those were quickly placed in a vacuum tube furnace with a vacuum degree of 10<sup>-3</sup> Pa. The reaction temperature of Zn and stainless steel was 360 °C, and the reaction time was 6 h, 12 h, 36 h and 48 h, respectively.

In order to observe the cross-section morphology of Fe-Zn compounds after reaction, the samples were corroded with 5 vol.% HNO<sub>3</sub>-2 vol.% HCl-93 vol.% alcohol solution. The morphology and elemental composition of the Fe-Zn intermetallics were analyzed by linkage between Zeiss Supra55 scanning electron microscope (SEM) and OXFORD energy dispersive X-ray spectroscopy (EDX). In order to characterize the degree of interaction between Zn and stainless steel, the thickness of compound was measured by Imagepro-Plus image analysis software. Each sample was measured 3 ~ 5 times to ensure the accuracy of the experimental results.

The characteristics of the passivation film produced by air passivation and chemical passivation were detected in the experiment. The composition and valence state of the passivation film on stainless steel were analyzed by XPS spectroscopy (Thermo ESCALAB 250Xi), and X-rays of Al K alpha (1486.6 eV, 15 kV and 14.9 mA) were used as the excitation source. The calibration error was +0.1 eV. The electrochemical Mott-Schottky test was carried out at CS350 type electrochemistry workstation. The sample was tested with three electrode systems in 3.5% NaCl solution, wherein the saturated calomel electrode (SCE) was the reference electrode, the platinum electrode was the auxiliary electrode, the passivation stainless steel was the working electrode. The effective area of stainless steel sample was 0.942 cm<sup>2</sup>. Scanning scope of Mott-Schottky tests was 0.5 V (SCE) ~ -1.5 V (SCE). The alternating

current signal was 10 mV, frequency was 1 kHz and step length was 25 mV in capacitance measurement.

### 3. RESULTS

#### 3.1 Interfacial intermetallics

Fig. 1 shows the cross section morphology of intermetallics (IMC) for the interaction between solid Zn and 304L SS with 24 h exposure in air. An interfacial compound layer is observed between the stainless steel and Zn. The layer with thickness of approximately 25  $\mu\text{m}$  is grown near Zn side. Meanwhile, the IMC thickness is nearly 1  $\mu\text{m}$  near the stainless steel side. To clearly observe the compound the morphology, the enlarged cross section morphology at  $\alpha$  is shown in Fig. 1(b). The flat compound is grown near the Zn side, wherein its composition is measured as 9.55 at.% Fe, 2.34 at.% Cr, 2.00 at.% Ni and 86.12 at.% Zn by EDX. Combined with the results of XRD analysis [15], this interfacial layer is characterized by  $\zeta$  phase,  $(\text{Fe, Cr, Ni})\text{Zn}_{13}$ . The acicular compounds grown near the steel substrate are composed of 28.14 at.% Fe, 24.25 at.% Cr, 1.32 at.% Ni and 46.29 at.% Zn. The compounds are  $\delta$  phase,  $(\text{Fe, Cr, Ni})\text{Zn}_{10}$ . This result is in accordance with the growth compounds reported in literature [16].

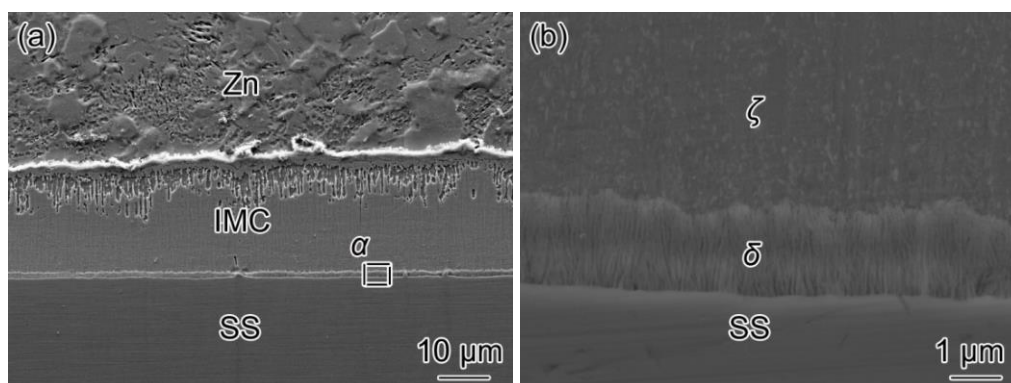
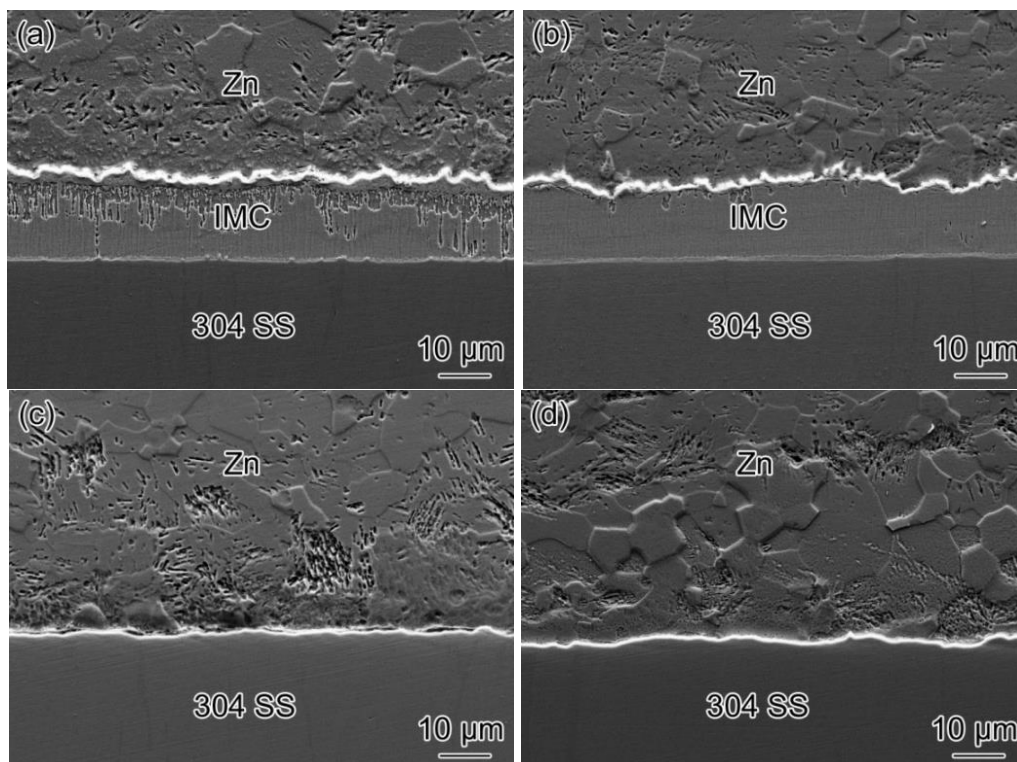


**Figure 1.** (a) Cross section microstructure of Fe-Zn intermetallics formed on stainless steel passivated in air for 24 h for 12 h reaction, (b) macromorphology of  $\alpha$  in Fig. (a)

#### 3.2 Effect of passivation film on IMC layer

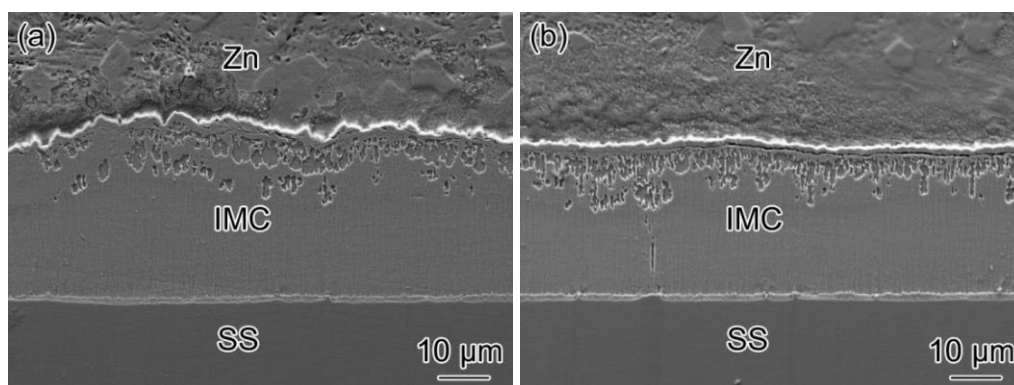
Figure 2 shows the IMC cross section microstructure of 304L stainless steel in different passivation states interacting with solid Zn for 6 h. A metallurgical layer is observed with 15  $\mu\text{m}$  thickness grown on 304L SS for 0 exposure in air. The compound layer near the stainless steel is too thin to distinguish its morphology. In Fig. 2(b), when stainless steel is passivated in air for 1 h, the IMC layer thickness is approximately is about 10  $\mu\text{m}$ . This value is less than that of the interface layer, as shown in Fig. 2(a). The interface compound layer cannot be observed in the interface of solid Zn and stainless steel from the exposure in air for 24 h sample and chemical passivation sample (shown in Fig. 2c and d, respectively). According to the above experimental results, an interfacial compound metallurgical layer can grow through the interaction of solid Zn and 304L SS. The oxide film in air for 1 h can hinder the

growth of Fe-Zn compound. No IMC layer exists on stainless steel with exposure in air for 24 h or chemical passivation.



**Figure 2.** Cross section microstructure of Fe-Zn intermetallics formed on different passivation 304L SS for 6 h reaction, (a) exposure in air for 0 h, (b) exposure in air for 1 h, (c) exposure in air for 24 h, (d) chemical passivation

Increasing the interaction time to 12 h, the cross section morphology of interface layers is shown in Fig. 3. Fe-Zn compound is observed on samples with air exposure for 0 h, 1 h and 24 h, shown in Fig. 3 (a), (b) and (c), respectively. In Fig. 3 (d), for chemical passivation stainless, no IMC is grown. For 12h interaction, not only the thickness of  $\zeta$  phase (Fe, Cr, Ni) $Zn_{13}$  near Zn increases, but also a thin compound layer appears near stainless steel substrate, as shown in Fig. 1.



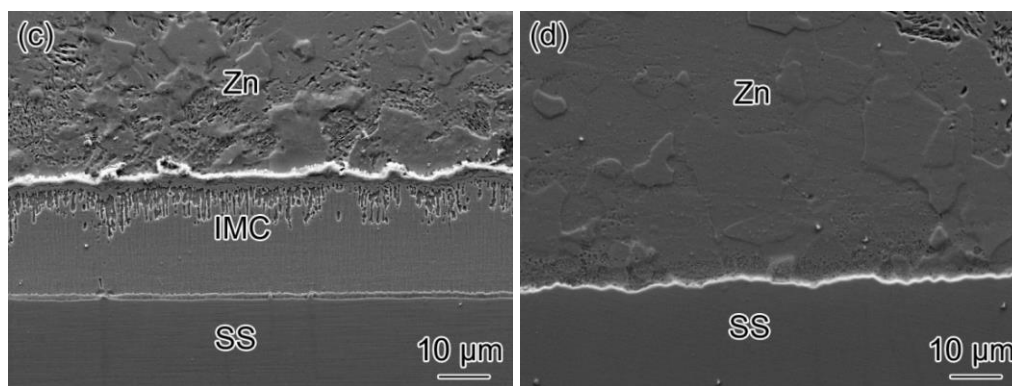


**Figure 3.** Cross section microstructure of Fe-Zn intermetallics formed on different passivation 304L SS for 12 h reaction, (a) exposure in air for 0 h, (b) exposure in air for 1 h, (c) exposure in air for 24 h, (d) chemical passivation

The cross section microstructure of Fe-Zn intermetallics formed after the reaction of samples with different passivation states with solid Zn for 36 h is shown in Fig. 4. It can be obtained that  $\zeta$  phase and  $\delta$  phase compounds continue to grow on stainless steel for air exposure, as shown in Fig. 4 (a), (b) and (c). It should be noted that in Fig. 4 (d), discontinuous growth compound appears at the interface of stainless steel treated by chemical passivation after contacting with Zn with more time. The chemical passivation film couldn't completely inhibit the metallurgical reaction of low melting point metal Zn with stainless steel, which results in the local growth of interfacial compounds.

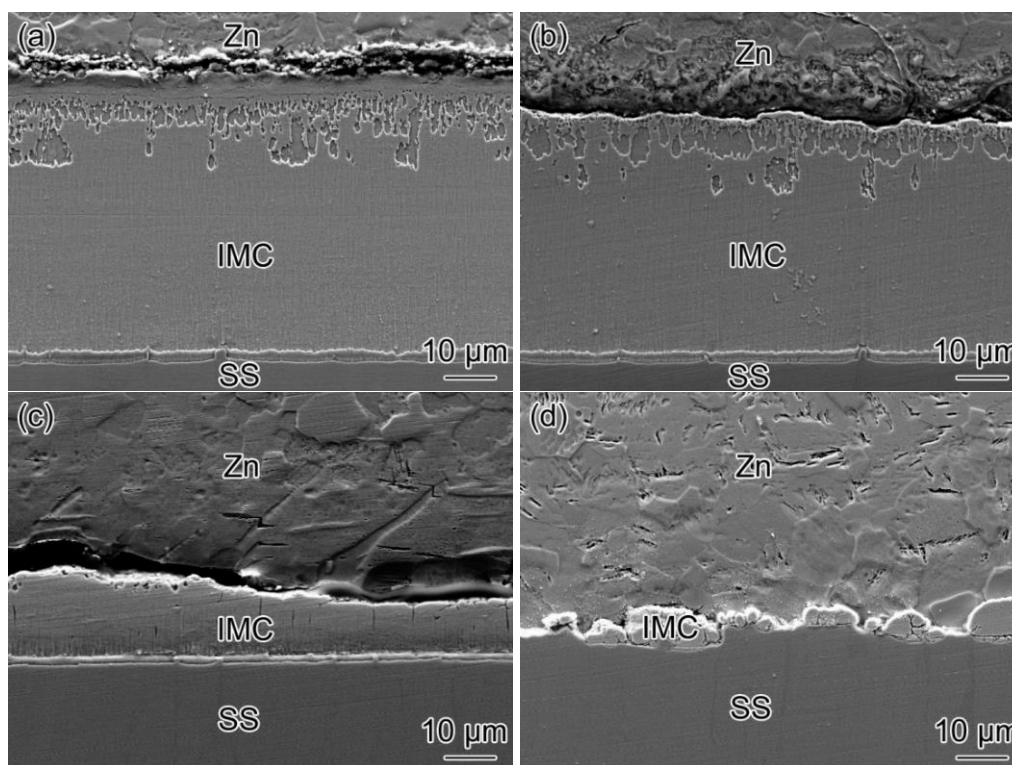


**Figure 4.** Cross section microstructure of Fe-Zn intermetallics formed on different passivation 304L SS for 36 h reaction, (a) exposure in air for 0 h, (b) exposure in air for 1 h, (c) exposure in air for 24 h, (d) chemical passivation

The cross section microstructure of the compounds formed in samples of different passivation states for 48 h reaction is shown in Fig. 5. The thickness of IMC metallurgical layer increases for more interaction time on air exposed stainless steels shown in Fig. 5 (a), (b) and (c) respectively. An interface Fe-Zn compounds grows inhomogeneously when sample with chemical passivation film, as shown in Fig. 5 (d). According to the above analysis, it is conferred that the thickness of the compound decreases gradually with the increasing air exposure time, and that the formation of intermetallics could be hindered by chemical passivation in a relatively short time. When the contact time between stainless steel and solid Zn was increased to 36 h, the local growth of IMC metallurgical layer is obtained.

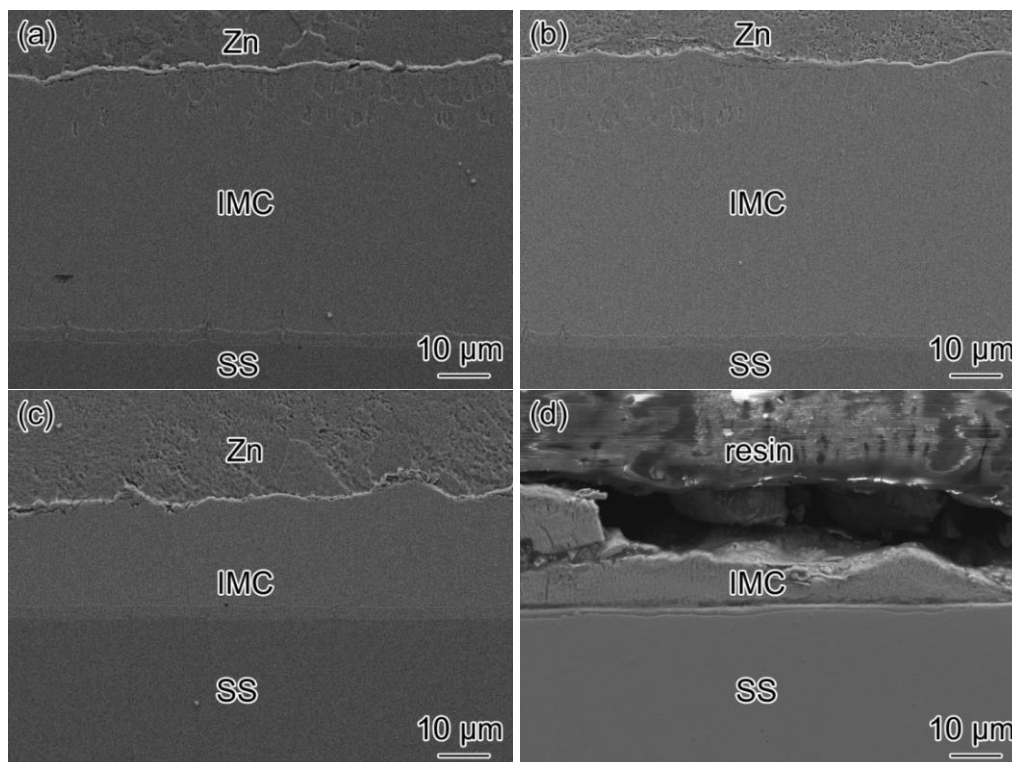


**Figure 5.** Cross section microstructure of Fe-Zn intermetallics formed on different passivation 304L SS for 48 h reaction, (a) exposure in air for 0 h, (b) exposure in air for 1 h, (c) exposure in air for 24 h, (d) chemical passivation

The relationship between the thickness and reaction time of the compound formed by the interaction of 304L stainless steel with solid Zn is described in Fig. 6. At air exposures of 0 and 1 h, the figure shows that the thickness of the compound increases gradually with the prolonged reaction time. However, the thickness increases slightly after the reaction time exceeds 36 h. At air exposure of 24 h, no interfacial compound layer forms within the 6 h reaction, and approximately 30 μm thick compound metallurgical layer grows when the reaction time increases to 12 h. When the reaction time continues to increase, the compound thickness does not remarkably change. No metallurgical compound layer is observed in the sample with chemical passivation within 12 h reaction. When the reaction time increases to 36 h, the compound is grown at the local interface. The local compound continues to grow when the reaction time increases to 48 h. The results of thickness characterization show that the interaction

between 304L stainless steel and solid Zn is influenced by the passivation films. The passive film on stainless steel exposed in air for 1 h has no obvious hindrance to the interaction. Fe-Zn metallurgical bonding layer is inhibited by passivation film at an air exposure time of 24 h and the reaction time of more than 6 h. With the increase of the reaction time, the continuous growth trend of the compound is not obvious. The passivation film can hinder the interaction when the reaction time is less than 24 h. The Zn atom and metal atoms of stainless steel pass through the passivation film, and the interdiffusion reaction occurs to grow the IMC compounds after 36 h contact. When the reaction time is longer than 36 h, the compound grows slowly. Air exposure for a long time or chemical passivation cannot prevent the interaction between stainless steel and solid Zn, but to some extent inhibits the growth of Fe-Zn compounds.

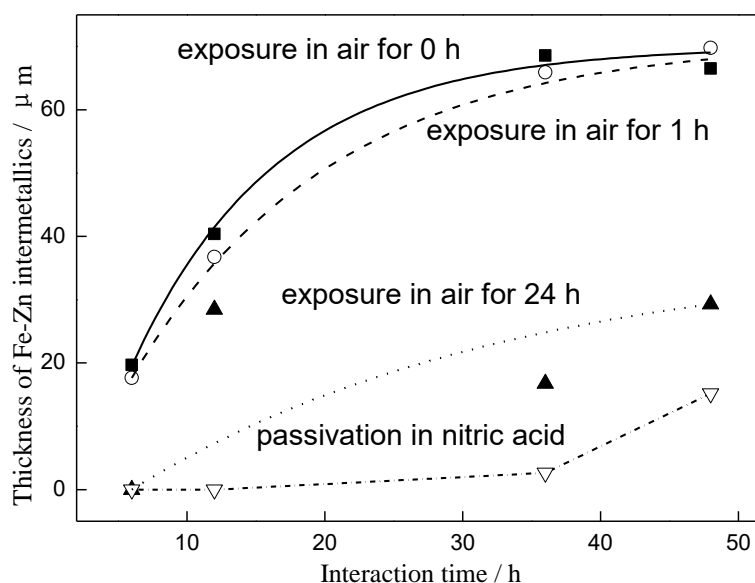


**Figure 6.** Thickness evolution of Fe-Zn intermetallics on different passivation 304L SS

## 4. DISCUSSION

### 4.1 Characteristics of passivation film

The composition of passive films grown in air and in hot HNO<sub>3</sub> is detected by XPS energy spectrometry. The experimental results are shown in Fig. 7. The peaks of Cr<sup>3+</sup> oxide [Cr<sup>3+</sup> (ox) 576 eV], Cr<sup>3+</sup> hydroxide [Cr 3 hydrous 577.3 eV], Cr<sup>6+</sup> oxide [Cr<sup>6+</sup> (ox) 578.4 eV] and metal Cr [Cr (met) 574.1 eV] are shown from the Cr 2p<sub>3/2</sub> high resolution diagram of Fig. 7 (a). Notably, Cr oxides and hydroxides occur in the passivation film. The Cr peak is the weakest in chemical passivation sample and increases with the decrease of air exposure time, whereas the peak of Cr rich oxide in the passivation film is the opposite to that of Cr. High-resolution map of Fe 2p<sub>3/2</sub> distinguishes the peak of Fe [Fe(met) 706.8 eV], Fe<sup>2+</sup> oxide [Fe<sup>2+</sup>(ox) 708.6 eV], Fe<sup>3+</sup> oxide [Fe<sup>3+</sup> (ox) 710.6 eV], Fe<sup>3+</sup> hydroxide [Fe<sup>3+</sup> (hyd) 711.8 eV], as shown in Fig 7(b). Remarkably, the passivation film contains Fe rich oxides and hydroxides. In Fig.

7(b), the O Spectrum (530.1 eV and 531.8 eV) is derived from metal oxides and adsorbs oxygen from air. The relative concentrations of Cr and Fe atoms in the passivation film are calculated according to the XPS spectra. The calculated results are shown in Table 2. The oxide peak can be observed on stainless steel exposed in air for 0 h, indicating that the self-passivation characteristic of stainless steel makes the oxide film form rapidly after the sample is polished. With the increase of air exposure time increases, the value of  $\{[Cr_{ox}]+[Cr_{hyd}]\}/\{[Cr_{ox}]+[Cr_{hyd}]+[Cr_{met}]\}$  change slightly and that of  $\{[Fe_{ox}]+[Fe_{hyd}]\}/\{[Fe_{ox}]+[Fe_{hyd}]+[Fe_{met}]\}$  increases. Based on the above results, Cr rich oxides and hydroxides are rapidly formed and stabilized in early stages after air self-passivation, and that Fe rich oxides and hydroxides grow gradually during air exposure.

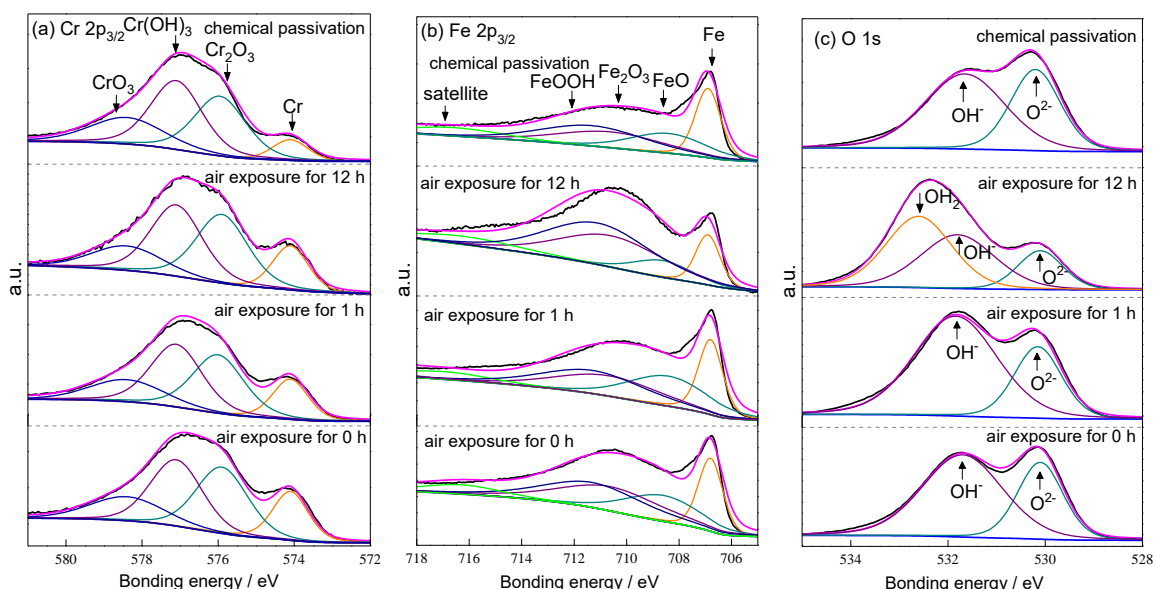


**Figure 7.** XPS spectra for passive films on 304L SS after air exposure and chemical passivation in HNO<sub>3</sub> solution, (a) Cr 2p<sub>3/2</sub>, (b) Fe 2p<sub>3/2</sub> and (c) O 1s

**Table 2.** Relative atomic concentrations calculated from XPS spectra for 304L SS after exposure in air and chemical passivation in HNO<sub>3</sub> solution

Relative atomic concentration	Air exposure			Chemical passivation
	0 h	1 h	12 h	
$\{[Cr_{ox}]+[Cr_{hyd}]\}/\{[Cr_{ox}]+[Cr_{hyd}]+[Cr_{met}]\}$	0.81	0.83	0.85	0.92
$\{[Fe_{ox}]+[Fe_{hyd}]\}/\{[Fe_{ox}]+[Fe_{hyd}]+[Fe_{met}]\}$	0.78	0.77	0.88	0.71
$\{[Cr_{ox}]+[Cr_{hyd}]\}/\{[Fe_{ox}]+[Fe_{hyd}]\}$	0.50	0.60	0.40	1.86
$[O^{2-}]/[OH^-]$	0.50	0.40	0.40	0.7

The relative atomic concentration of the passive film was observed on chemical passivation stainless steel. The experimental results of Table 2 showed that the concentration of Cr oxide and hydroxides in chemical passivation film was relatively higher than that of air oxide film.

{[Crox]+[Crhyd]}/{[Feox]+[Fehyd]} of the former is nearly 30% higher than that of the latter. The experimental results of XPS indicated that the chemical composition of passivation film between air exposure treatment and chemical passivation treatment was different, and Cr oxides and hydroxides were richer in chemical passivation film than oxide film in air.

Mott-Schottky test is used to analyze the semiconductor characteristics of oxide film in air and chemical passivation film. By measuring the relationship between the electrode capacitance  $C$  and the electrode potential  $E$ , the distribution of the charge in passivation film is obtained as follows:

$$\frac{1}{C^2} = \frac{2}{\epsilon\epsilon_0 eAN_D} \left( E - E_{FB} - \frac{kT}{e} \right) \quad \text{n-type semiconductor} \quad (1)$$

$$\frac{1}{C^2} = \frac{-2}{\epsilon\epsilon_0 eAN_A} \left( E - E_{FB} - \frac{kT}{e} \right) \quad \text{p-type semiconductor} \quad (2)$$

Where  $E$  is applied potential  $V_{SCE}$ ,  $e$  is electron charge,  $\epsilon$  is dielectric constant,  $\epsilon_0$  is vacuum dielectric constant ( $F\text{ cm}^{-1}$ ),  $A$  is electrode surface area,  $K$  is Boltzmann's constant,  $T$  is absolute temperature,  $E_{FB}$  is flat band potential  $V_{SCE}$ .  $N_D$  and  $N_A$  are n-type semiconductor donor concentration and p-type semiconductor acceptor concentration( $\text{cm}^{-3}$ ), respectively.

Figure 8 shows the Mott-Schottky test results of 304L stainless steel at different passivation states. The experimental potential ranges from 0.5  $V_{SCE}$  to -1.5  $V_{SCE}$ , which is consistent with the test parameters reported in literature [17]. The capacitance of 304L stainless steel exposed in air for 0 h is higher than that of air exposure or of chemical passivation samples. The slope of Mott-Schottky curve is positive when potential is in the range of -0.2 ~ 0.2  $V_{SCE}$ , and the slope of the curve is negative when potential is in the range of -1.15 ~ -0.89  $V_{SCE}$  (air exposure sample) or -1.35 ~ -0.89  $V_{SCE}$  (chemical passivation sample). The positive slope indicates that the oxide is n-type semiconductor, whereas the negative slope indicates that the oxide is p-type semiconductor.

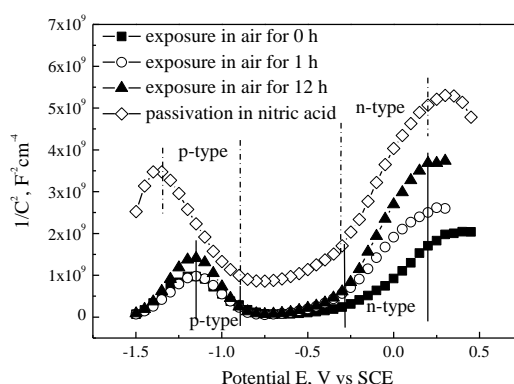


**Figure 8.** Mott-Schottky plots for different passivation 304L SS in 3.5 % NaCl solution

The semiconductor behavior characteristic of stainless steel indicates that passive film is a bilayer structure, wherein the outer layer is mainly Fe-rich oxide with n-type semiconductor structure, whereas the inner layer is mainly composed of Cr-rich oxide with p-type semiconductor structure [18]. According

to reference [19], the relative dielectric constant in formula (1) and (2) is 12. The donor concentration  $N_D$  of positive potential region and the acceptor concentration  $N_A$  of negative potential region can be calculated by the slope of straight line region. The results are shown in Table 3. The values of  $N_D$  and  $N_A$  are in the order of  $10^{21} \text{ cm}^{-3}$ , which is within the range reported in [20]. Compared with that of the fresh surface stainless steel, the donor concentration  $N_D$  of oxide film in air is reduced by 24 % -50 %, whereas its acceptor concentration  $N_A$  is almost identical. However, the donor concentration  $N_D$  and the acceptor concentration  $N_A$  of chemical passivation are low. The experimental results of Mott-Schottky test of stainless steel at different passivation states show that the donor concentration and acceptor concentration of passivation film grown by air self-passivation and chemical passivation are obviously different. This result is related to the composition difference of Cr、 Fe oxide in the passivation film and the passivation film integrity.

**Table 3.** Doping density for different passivation 304L SS in 3.5 % NaCl solution

	304L SS exposed in air			Chemical passivation in HNO <sub>3</sub> solution
	0 h	1 h	12 h	
$N_D (10^{21} \text{ cm}^{-3})$	3.56	2.68	1.75	1.7
$N_A (10^{21} \text{ cm}^{-3})$	4.37	4.51	4.29	1.9

The composition difference of passivation film of stainless steel grown in oxidizing environment was reported in [21]. Wegrelius and Sjoden suggested that the Cr/Fe ratio of passivation film grown by nitric acid passivation is high, and the corrosion resistance of stainless steel is improved. This result was due to the selective dissolution of Fe atoms in the passivation film grown by nitric acid passivation treatment on stainless steel; this phenomenon increased the Cr atom content in the passivation film. Literature [22] also reported that the Fe rich oxide film on the surface of stainless steel is loose and not compact, providing a diffusion channel for external ions. Fe rich oxide film cannot effectively protect the stainless steel substrate. Vayer [23] argued that the passive film formed spontaneously in air was mainly composed of Fe oxide and Cr oxide is rare in the film, and that the Cr-rich oxide is the main component of the passivation film passivated by HNO<sub>3</sub>. Cr-rich oxide in passivation film is the main component protecting stainless steel from external erosion [24]. Therefore, the difference of Cr/Fe ratio between the oxidation film grown by air self-passivation and the chemical passivation film is one of the reasons why their donor concentration and acceptor concentration of passivation film are significantly different. The difference of donor concentration  $N_D$  and acceptor concentration  $N_A$  in passivation film is related to the disordered arrangement of atoms or the incompleteness of space charge [25]. High  $N_D$  and  $N_A$  values indicate that the passivation film is incomplete and cannot effectively prevent the direct contact between the external ions and the stainless steel substrate. Compared with air exposure stainless steel, the donor concentration and acceptor concentration of the chemical passivation sample are obviously lower than those of stainless steel exposed in air. This finding indicates that the passivation film is relatively complete grown by chemical passivation.

#### 4.2 Interaction mechanism

Based on the results of XPS and Mott-Schottky mentioned previously, the integrity evolution of passivation film on stainless steel surface after air exposure and chemical passivation treatment was summarized. Rare thin passivation film was observed on the surface of stainless steel simply after mechanical grinding. Incomplete passivation film was formed after exposure in air for 1 h. The inner film layer was mainly Cr rich oxide, and the outer layer was mainly Fe rich oxide. When air exposure time of stainless steel was increased to 12 h, the oxides rich in Cr and Fe grew gradually. Cr rich Oxides in the inner layer grew slowly after 24 h exposure in air, but Fe rich oxides in the outer layer continued to grow. However, the outer Fe-rich oxides were loose and porous, and the passive films grown on stainless steel surface were still incomplete. Passivation film formed on stainless steel by chemically passivation was composed of a dense oxide rich in Cr in the inner layer, and a loose oxide rich in Fe in the outer layer. Moreover, the oxide rich in Cr was the main component of the film.

Passivation film on stainless steel surface hinders the interaction between low-melting-point-metal and stainless steel. The passivation film is composed of bilayer oxide, wherein oxide rich in Fe is in the outer layer and oxide rich in Cr is the inner layer. According to Ma et al [26], it is argued that the Cr oxide is a physical barrier to inhibit the formation of intermetallic compound on stainless steel surface. Jordan C E [27] reported that Fe oxides can prevent the interaction of liquid metals with steel. Our results showed that the oxidation film grown in air and in HNO<sub>3</sub> solution hinders the growth of Fe-Zn intermetallic compounds in varying degrees. The evolution of interfacial compounds with reaction time is shown in Fig. 9. In the initial stage, low-melting point metal Zn can easily contact with stainless steel due to the inhomogeneous and incomplete passivation film growing on stainless steel surface (Fig. 9a). The low melting point metal atom and metal atom both pass through the passivation film barrier and exhibits the diffusion reaction (Fig. 9b). Meanwhile, the intermetallic compound forms and grows gradually, and the discontinuous passivation film is still in the interface layer (Fig. 9b). When interaction time increases, the chemical driving force generated by the gradual growth of the interface compound leads to rupture of the passivation film, which is randomly embedded in the compound or the low-meltingpoint metal (Fig. 9d). Low-melting point metal can interact with stainless steel to form IMC compound due to incomplete passivation film. This phenomenon cannot inhibit atom diffusion. However, compact passivation film can restrain the formation and growth of intermetallic compound to some extent. The diffusion between low-melting point metal and stainless steel substrates is restrained due to the passivation film as a physical barrier.

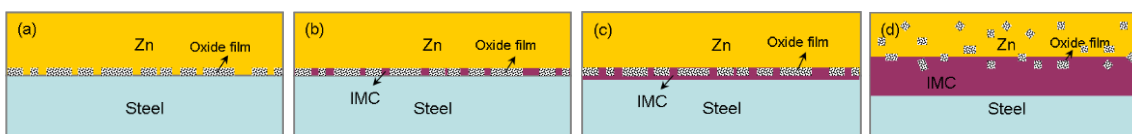


**Figure 9.** Schematic illustration of the effect of the passive film on the interaction between low melting point metals and stainless steels

#### 4. CONCLUSION

(1) XPS and Mott-Schottky measurements were used to analyze the characteristics of passivation film on stainless steel surface. The passivation film is composed of oxides rich in Fe and Cr and hydroxides. The chemical passivation film enriches more oxides of Cr and hydroxide than air passivation film. By increasing the exposure time in air, the donor concentration  $N_D$  decreased, whereas the acceptor concentration  $N_A$  remained unchanged. By contrast, for the chemical passivation stainless steel, the donor concentration  $N_D$  and the acceptor concentration  $N_A$  was obviously low. This result indicates that the chemical passivation film is more complete than oxide film in air.

(2) The interaction between solid Zn and passivated stainless steel involved the formation of  $\zeta$  phase (Fe, Cr, Ni) $Zn_{13}$  and  $\delta$  phase (Fe, Cr, Ni) $Zn_{10}$  interface compounds. The compound thickness is reduced by the passivation film grown on the surface. The passivation film acts as a physical barrier to some extent to inhibit the diffusion reaction between Zn atoms and stainless steel substrate. The block effect of chemical passivation film on the growth of compounds is more remarkable than that of air self-passivation oxide film.

#### ACKNOWLEDGMENT

This work was supported by National Nature Science Foundation of China (NSFC No. 51571051), Science and Technology Research Fund of Liaoning Province Department of Education (NO. L2016008 and L2017LQN026), Dr Research Start-up Fund of Liaoning Province (No. 201601336) and Scientific Research Cultivation Fund of LSHU (No.2016PY-024).

#### References

1. J. Luo, H. Cheng, K.M. Asl, Y.C.J. Kiel, M.P. Harmer, *Science*, 1730 (2011), 333.
2. T. Auger, Z. Hamouche, A. Medin, D. Gorse, *J. Nucl. Mater.*, 253 (2008),377.
3. Deming Xie, Jiming Hu, Shaoping Tong, Jianming Wang, Jianqing Zhang, *Acta Metall. Sin.*, 103 (2004) 1.
4. Qiang Hu, Anguo Huang, Zhongsuo Li, *Electronic industrial specialized equipment*, 53 (2005), 34.
5. G.M., Song, T. Vystavel, N. Vanderpers, J.T.M. De Hosson, W.G. Sloof, *Acta Mater.*, 6, (2012) 2973.
6. G. Reumont, J.B. Vogt, A. Iost, J. Foct, *Surf. Coat. Tech.*, 139 (2001) 265.
7. E.M. Bellhouse, J. R. Mcdermin, *Mat. Sci. Eng. A*, 491 (2008) 39.
8. S. Ma, J.Xing, H. Fu, D. Yi, *Corros. Sci.*, 53 (2011) 2826.
9. J.D. Culcasi, P.R. Sere, C.I. Elsner, A.R.D. Sarli, *Surf. Coat. Tech.*, 122 (1999) 21.
10. R. Kainuma, K. Ishida, *ISIJ Int.*, 47 (2007) 740.
11. J. Lee, J. Park, S.H. Jeon, *Metall. Mater. Trans. B*, 40 B (2009) 1035.
12. American Society for Testing Materials. Philadelphia, United States: ASTM, 2006.
13. C.Q. Cheng, J. Zhao, T.S. Cao, Q.Q. Fu, M.K. Lei, D.W. Deng, *Corros. Sci.*, 70 (2013) 235.
14. ASME NQA-1:2004, Quality Assurance Requirements for Cleaning of Fluid Systems and Associated Components for Nuclear Power Plants.
15. Y. Zhao, C.Q. Cheng, Z.Y. Cao, J. Zhao, *Mater. Charact.*, 77 (2013) 1.
16. S.Q. Ma, J.D. Xing, D.W. Yi, H.G. Fu, S.C. Ma, *Mater. Charact.*, 61 (2010) 866.
17. N.E. Hakiki, *Corros. Sci.*, 53 (2011) 2688.

18. S. Marcelin, B.T. Ovanessian, B. Normand, *Electrochem. Comm.*, 66 (2016) 62.
19. X.M. Zhu, Y. Guo, Z.Q. Xing, M.K. Lei, *J. Electrochem. Soc.*, 159 (2012) C319.
20. X.G. Li, D.W. Zhang, Z.Y. Liu, Z. Li, C.W. Du, C.F. Dong, *Nature*, 527 (2015) 441.
21. L. Wegelius, B. Sjoden, *Outokumpu stainless steel*, 4 (2004) 1.
22. X. Wang, H.B. Xiao, *Int. J. Electrochem. Sci.*, 12 (2017) 268.
23. M. Vayer, I. Reynaud, R. Erre, *J. Mater. Sci.*, 35 (2000) 2581.
24. C.H. Wang, H.H. Chen, P.Y. Li, P.Y. Chu, *Intermetallics*, 22 (2012) 166.
25. A. Fattah-alhosseini, F. Soltani, F. Shirsalimi, B. Ezadi, N. Attarzadeh, *Corros. Sci.*, 53 (2011) 3186.
26. Y.H. Ma, A.B. Ceylan, A.M. Engin, F. Guazzone, E.E. Engwall, *Ind. Eng. Chem. Res.*, 43 (2004)2936.
27. C.E. Jordan, A.R. Marder, *Metall. Mater. Trans. B*, 29B (1998) 479.

© 2019 The Authors. Published by ESG ([www.electrochemsci.org](http://www.electrochemsci.org)). This article is an open access article distributed under the terms and conditions of the Creative Commons Attribution license (<http://creativecommons.org/licenses/by/4.0/>).